Metal–Organic Materials Hot Paper

International Edition: DOI: 10.1002/anie.201603934
German Edition: DOI: 10.1002/ange.201603934

Tuning Pore Size in Square-Lattice Coordination Networks for Size-Selective Sieving of CO_2

Kai-Jie Chen, David G. Madden, Tony Pham, Katherine A. Forrest, Amrit Kumar, Qing-Yuan Yang, Wei Xue, Brian Space, John J. Perry IV, Jie-Peng Zhang, Xiao-Ming Chen, and Michael J. Zaworotko**

Abstract: *Porous materials capable of selectively capturing CO_2 from flue-gases or natural gas are of interest in terms of rising atmospheric CO_2 levels and methane purification. Size-exclusive sieving of CO_2 over CH_4 and N_2 has rarely been achieved. Herein we show that a crystal engineering approach to tuning of pore-size in a coordination network, [Cu(quinoline-5-carboxyate)$_2$]$_n$ (**Qc-5-Cu**) ena+bles ultra-high selectivity for CO_2 over N_2 ($S_{CN} \approx 40000$) and CH_4 ($S_{CM} \approx 3300$). **Qc-5-Cu-sql-β**, a narrow pore polymorph of the square lattice (**sql**) coordination network **Qc-5-Cu-sql-α**, adsorbs CO_2 while excluding both CH_4 and N_2. Experimental measurements and molecular modeling validate and explain the performance. **Qc-5-Cu-sql-β** is stable to moisture and its separation performance is unaffected by humidity.*

Carbon dioxide (CO_2) is a greenhouse gas and an undesirable impurity that is a component of several industrially relevant gas mixtures. The concentration of CO_2 in the atmosphere surpassed 400 ppm for the first time in 2013[1] highlighting an urgent need for new solutions to CO_2 emissions. Moreover, the use of natural gas and biogas as cleaner alternatives to traditional fossil fuels is also increasing.[2] Natural gas upgrading and biogas sweetening require removal of CO_2 and other impurities. The current state-of-the-art with respect to carbon capture employs liquid amine chemisorbents such as primary and secondary alkyl amines. However, chemisorbents typically require energy-intensive regeneration processes and are often corrosive. Physisorbents also offer a potential solution since they can offer faster kinetics and more facile regeneration. Molecular sieving represents a third option for carbon capture but requires rigid networks with pore apertures intermediate between the kinetic diameters of the species to be separated. Metal–organic materials (MOMs),[3] also known as porous coordination polymers[4] or metal–organic frameworks (MOFs),[5] can enable exquisite control over pore-size and pore-chemistry thanks to their inherent modularity, especially if prototypal for families of closely related MOMs.

Crystal engineering[6] or reticular chemistry[7] approaches to the generation of families of MOMs can offer control over pore dimensions and chemistry in a manner that is difficult to achieve in existing classes of porous materials. Indeed, new selectivity benchmarks for polarizable sorbates (e.g. CO_2) have been realized by adjusting pore-size to around that of the sorbate and through the use of inorganic linkers that offer strong electrostatics.[8] Control over pore-size in these hybrid ultra-microporous (< 0.7 nm) materials can be achieved through short organic linkers or interpenetration.[8a,9]

Molecular sieving can enable ultra-high selectivity by excluding species with kinetic diameters larger than the pore (e.g. $N_2 = 3.64$ Å; $CH_4 = 3.8$ Å) while allowing passage of smaller guests (e.g. $CO_2 = 3.3$ Å). Unfortunately, molecular sieving has rarely been achieved,[10] largely because it is difficult to control pore-size within the 3–4 Å range that is most relevant for gas molecule separations.[11] Further, defining a material to be a molecular sieve after observing a large uptake difference for two adsorbates at low temperatures (e.g. 195 K CO_2 vs. 77 K N_2) could be an artifact of pore contraction, slower gas diffusion rates or reduced thermal motion. Indeed, dynamics are unwanted in sieving materials as they could induce a gate-opening effect and lost sieving ability. To our knowledge, there are only a handful of molecular sieves for CO_2 over CH_4 and/or N_2 at or near ambient conditions.[12] In addition, as yet uncharacterized activated structures can account for the observed molecular sieving in several of these examples. We also note that coordination networks invariably exhibit preference towards CO_2 over N_2 and/or CH_4 because of weak adsorbate-adsorbent interactions. CO_2/N_2 selectivity, S_{CN}, rarely exceeds 100 in such materials.

Herein, we report that fine-tuning of pore-size enables molecular sieving of CO_2 thanks to supramolecular isomerism, that is, the generation of networks with the same chemical composition, but different topology.[6,13] Five coordination networks of formula [M(quinoline-5-carboxyate)$_2$]$_n$, **Qc-5-M-dia** (**M** = Co, Ni, Zn and Cu, **dia** = 2-fold, 3D diamondoid network) and **Qc-5-Cu-sql-α** (**sql** = 2D square lattice network), were synthesized solvothermally from HQc (quinoline-5-carboxylic acid) and the respective metal salts

[*] Dr. K.-J. Chen, Dr. D. G. Madden, A. Kumar, Dr. Q.-Y. Yang, Dr. J. J. Perry IV, Prof. Dr. M. J. Zaworotko
Department of Chemical & Environmental Sciences, Bernal Institute
University of Limerick
Plassey House, Limerick (Republic of Ireland)
E-mail: Michael.Zaworotko@ul.ie
Dr. K.-J. Chen, Dr. W. Xue, Prof. Dr. J.-P. Zhang, Prof. Dr. X.-M. Chen
MOE Key Laboratory of Bioinorganic and Synthetic Chemistry, School of Chemistry and Chemical Engineering
Sun Yat-Sen University
Guangzhou 510275 (P.R. China)
E-mail: zhangjp7@mail.sysu.edu.cn
Dr. T. Pham, K. A. Forrest, Prof. Dr. B. Space
Department of Chemistry, University of South Florida
4202 E. Fowler Ave., CHE205, Tampa, FL 33620-5250 (USA)

Supporting information for this article can be found under: http://dx.doi.org/10.1002/anie.201603934.

(see Supporting Information). **Qc-5-Cu-dia** and **Qc-5-Cu-sql-α** are supramolecular isomers. These materials were studied by single-component gas sorption, dynamic breakthrough of gas mixtures, temperature-programmed desorption (TPD), and molecular modeling. In the process we observed that **Qc-5-Cu-sql-α** undergoes an irreversible phase change upon desolvation to **Qc-5-Cu-sql-β**, a more stable polymorph of **Qc-5-Cu-sql-α**. The β-phase does not revert back to the α-phase even after attempted re-solvation (see Figure 2), heating or soaking in water for 21 days. Interestingly, **Qc-5-Cu-sql-β** adsorbs moderate quantities of CO_2 at 293 K and 1 atm, but little CH_4 or N_2 under the same conditions, suggesting a sieving effect.

Qc-5-M-dia crystallizes as 2-fold interpenetrated **dia** networks in tetragonal space groups whereas **Qc-5-Cu-sql-α** crystallizes in the monoclinic space group $P2_1/c$ (Figure 1, Table S1). The coordination geometry around the metal cations is distorted octahedral: each metal is coordinated to four oxygen atoms (from two carboxylate groups) and two nitrogen atoms (from two quinoline rings). Different orientations of the linker ligand (Table S2 in the Supporting Information) enables supramolecular isomerism to occur in **Qc-5-Cu. Qc-5-Cu-dia** and **Qc-5-Cu-sql-α** exhibit 1D channels with diameters of 4.8 Å and 3.8 Å, respectively, and network void spaces of 34.7% and 23.5%, respectively, as calculated by Platon.[14] The purity of as-synthesized and activated bulk samples was validated by powder X-ray diffraction (PXRD; Figure 2 and Figures S5–S8). Thermogravimetric analysis (TGA) measurements reveal that solvent molecules are released well before network decomposition occurs at approximately 240 °C and 280 °C, respectively, for **Qc-5-Cu-dia** and **Qc-5-Cu-sql-α** (Figure S12). **Qc-5-Co-dia** and **Qc-5-Zn-dia** both undergo structural changes to unknown amorphous phases; as such, neither compound was subjected to further study. For **Qc-5-Cu-sql-α**, we noted that PXRD patterns collected before and after desolvation at 130 °C suggest a phase transformation. Single-crystal X-ray diffraction data collected on a desolvated crystal of **Qc-5-Cu-sql-α**, that is, **Qc-5-Cu-sql-β**, reveal that space group and topology are retained. However, the *a*- and *c*-axes contract, along with the cell volume (1004.1 ± 0.1 to 908.0 ± 0.1 Å^3), calculated void space (23.5% to 17.2%) and pore-size (3.8 to 3.3 Å). The stacking of **sql** networks in **Qc-5-Cu-sql-β** is controlled by π–π interactions between quinoline moieties from adjacent layers and interlayer quinoline to carboxylate C–H···O interactions. The torsion angle of the quinoline ring with respect to the square plane of the metal centers in **Qc-5-Cu-sql-β** is bigger than that of **Qc-5-Cu-sql-α**, consistent with the observed pore-size contraction. Concomitantly, C–H···O distances in **Qc-5-Cu-sql-β** are shorter than those of **Qc-5-Cu-sql-α** (Figure S2). The pore-size in **Qc-5-Cu-sql-β** is approximately that of the kinetic diameter of CO_2 and therefore smaller than those of N_2 and CH_4. N_2 and CO_2 sorption isotherms were measured at 77 and 195 K, respectively, to determine if **Qc-5-Cu-sql-β** exhibits a sieving effect consistent with its pore-size. Very low uptake of N_2 (4.3 cm^3 g^{-1}) was observed at 77 K and 1 bar, which is consistent with surface

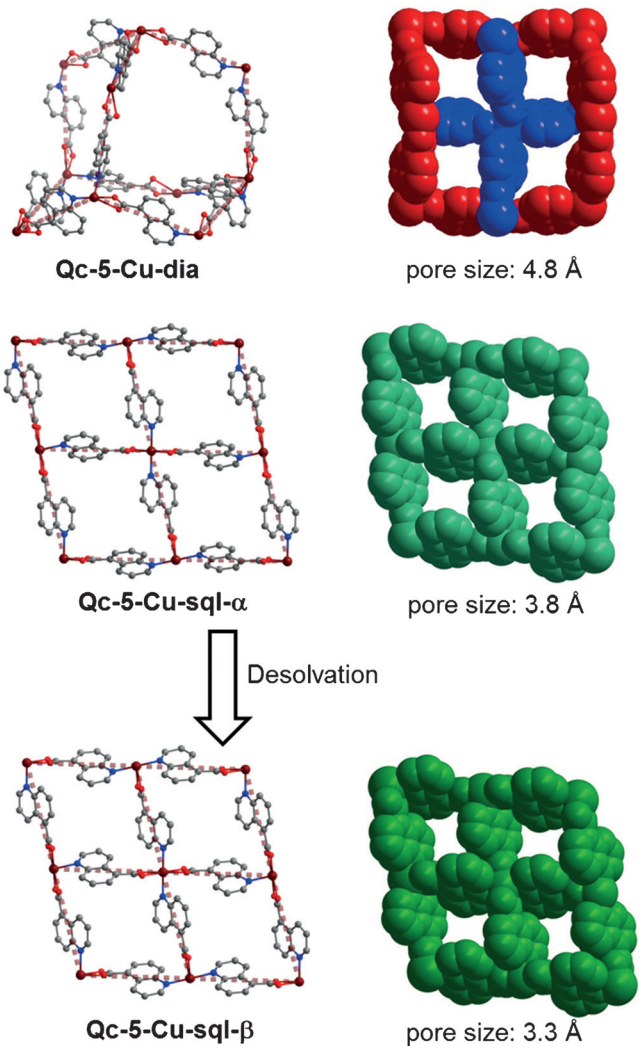

Figure 1. Pore-size tuning from supramolecular isomerism in diamondoid (**dia**, above) and square lattice (**sql**, below) polymorphs of $[Cu(Qc)_2]_n$.[23] C (gray), Cu (maroon), O (red), N (blue), H (white).

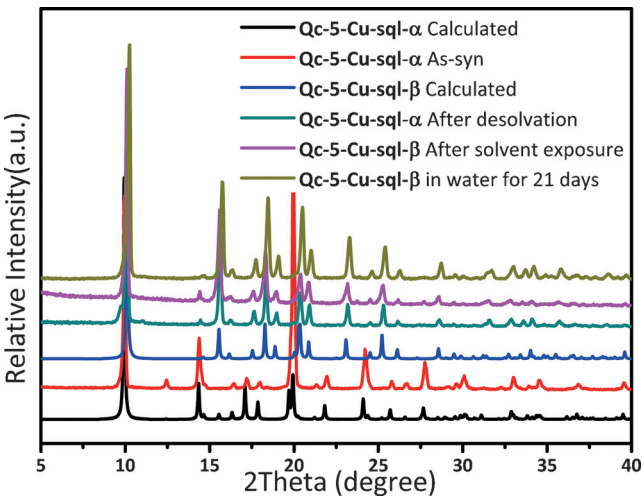

Figure 2. Calculated and experimentally measured PXRD patterns of **Qc-5-Cu-sql-α** and **Qc-5-Cu-sql-β** after exposure to solvent and water.

adsorption. CO_2 uptake of 59 $cm^3 g^{-1}$ at 195 K and 1 bar equates to an apparent BET surface area of 222 $m^2 g^{-1}$. CO_2, N_2, and CH_4 sorption experiments were conducted at 273, 283, and 293 K for **Qc-Ni-dia**, **Qc-5-Cu-dia** and **Qc-5-Cu-sql-β. Qc-5-Ni-dia** and **Qc-5-Cu-dia** exhibit 293 K and 1 bar uptakes of N_2 (7.1 and 5.8 $cm^3 g^{-1}$) and CH_4 (25.6 and 24.6 $cm^3 g^{-1}$) that are much larger than those of **Qc-5-Cu-sql-β** (N_2: 0.3 $cm^3 g^{-1}$, CH_4: 1.3 $cm^3 g^{-1}$; Figure 3). Conversely, **Qc-5-Cu-sql-β** exhibits a higher CO_2 uptake than even **Qc-5-Cu-dia** at 293 K and 1 bar. CO_2/N_2 (S_{CN}) and CO_2/CH_4 (S_{CM}) selectivities were calculated in two ways: ratio of uptakes determined from single-component isotherms; ideal adsorbed solution theory (IAST).[15] The very different sorption behavior that results from pore-size tuning means that S_{CN} (40000) and S_{CM} (3300) are much higher than **Qc-5-Cu-dia** (19 and 3), **Qc-5-Ni-dia** (36 and 7) and, more importantly, the vast majority of porous materials studied to date (Table 1, Table S3).[16] Details about sorption isotherm fitting and selectivity calculations are given in Figures S29–S39. CO_2 isotherms measured at 273, 283, and 293 K were fitted using the virial equation (Figures S23, S25 and S27), and the isosteric heat of adsorption (Q_{st}) was calculated using the Clausius–Clapeyron equation. **Qc-5-Cu-sql-β** exhibits a higher Q_{st} (36 kJ mol^{-1}) than **Qc-5-Ni-dia** (32 kJ mol^{-1}) and **Qc-5-Cu-dia** (34 kJ mol^{-1}). Such values are comparable to porous materials with polar functional moieties or unsaturated metal sites, such as NJU-Bai8 (38 kJ mol^{-1}),[12c] HKUST-1 (35 kJ mol^{-1}),[17] Bio-MOF-1 (35 kJ mol^{-1})[18] and PCN-6 (35 kJ mol^{-1}).[19] However, these values are lower than benchmark hybrid ultra-microporous materials (40–55 kJ mol^{-1}).[8]

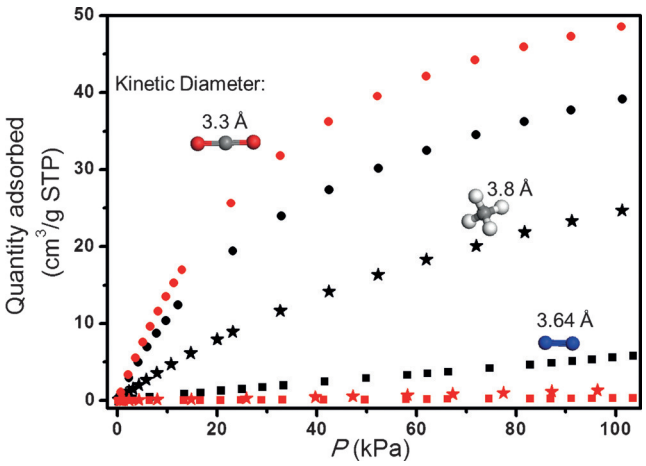

Figure 3. CO_2 (circle), CH_4 (star), and N_2 (square) sorption data at 293 K for **Qc-5-Cu-dia** (black) and **Qc-5-Cu-sql-β** (red).

To further understand the sorption behavior in **Qc-5-Ni-dia**, **Qc-5-Cu-dia**, and **Qc-5-Cu-sql-β**, molecular simulations of their CO_2 adsorption were performed. These studies reveal that closest interactions between CO_2 molecules and pore walls are from CO_2 oxygen atoms and the nearby H atoms of the Qc linkers. Indeed, the adsorbed CO_2 molecules are oriented such that the negatively charged CO_2 oxygen atoms can interact with the positively charged H atoms of the linkers. When comparing the modeled CO_2-loaded structure for **Qc-5-Cu-sql-β** with that for **Qc-5-M-dia**, the former was found to exhibit a better close-fitting interaction between CO_2 molecules and the pore walls (Figure 4 and Figure S48–S57). This is indicated by the significantly shorter O(CO_2)···H distances in **Qc-5-Cu-sql-β** relative to **Qc-5-Ni-dia** and **Qc-5-Cu-dia**. The distances between the CO_2 oxygen atoms and the H atoms of the Qc linkers is under 2.5 Å in **Qc-5-Cu-sql-β** and over 3.0 Å in **Qc-5-Ni-dia** and **Qc-5-Cu-dia** (Figure 4 and Figure S55).

Retention of structural integrity after exposure to water or water vapor is a requirement of any material that might be

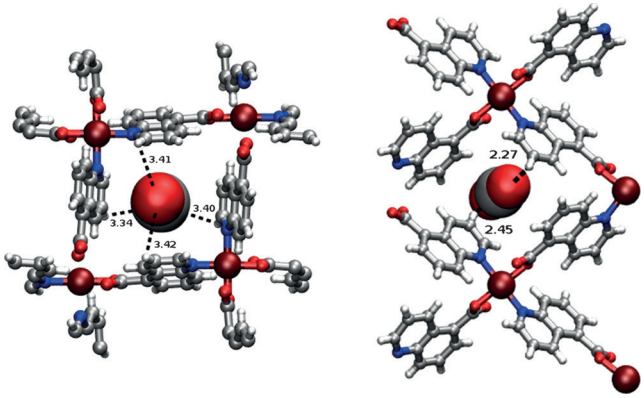

Figure 4. The modelled binding site in the CO_2-loaded structures of **Qc-5-Cu-dia** (left) and **Qc-5-Cu-sql-β** (right) within a unit cell and a 1×2×1 system cell, respectively. C (gray), Cu (maroon), O (red), N (blue), H (white).

Table 1: Summary of structural information and sorption data.

Compounds	Topology	Pore size [Å]	BET surface area [$m^2 g^{-1}$]	CO_2 uptake [$cm^3 g^{-1}$][d]	CH_4 uptake [$cm^3 g^{-1}$][d]	N_2 uptake [$cm^3 g^{-1}$][d]	Q_{st} of CO_2 [kJ mol^{-1}][e]	CO_2/H_2O captured[f]	S_{CM}[g]	S_{CN}[h]
Qc-5-Ni-dia	**dia**	4.8	664[b]	58.9	25.6	7.1	32	0.13	7/3	36/26
Qc-5-Cu-dia	**dia**	4.8	488[c]	39.2	24.6	5.8	34	0.53	3/2	19/16
Qc-5-Cu-sql[a]	**sql**	3.3	222[c]	48.4	1.3	0.3	36	1.35	3300/68	40000/463

[a] the desolvated phase of **Qc-5-sql**; [b] calculated from 77 K CO_2 isotherm; [c] calculated from 195 K CO_2 isotherm; [d] at 293 K and 1 bar; [e] Q_{st} at low loading; [f] the ratio of amounts of CO_2 and H_2O captured from wet flue gas mixture/(0.15/0.025); [g] left value: selectivity from IAST theory, right value: selectivity from CO_2 uptake at 0.5 bar/CH_4 uptake at 0.5 bar; [h] left value: selectivity from IAST theory, right value: selectivity from CO_2 uptake at (0.15 bar/N_2 uptake at 0.85 bar)/(0.15/0.85).

considered for industrial applications. Recently, we introduced "accelerated stability" pharmaceutical industry methods to evaluate the performance and stability of MOMs after exposure to water vapor.[20] **Qc-5-Cu-dia**, **Qc-5-Ni-dia**, and **Qc-5-Cu-sql-α, Qc-5-Cu-sql-β** were subjected to these methods and exposed to 75% humidity at 40°C for 1, 7, and 14 days. After 1 day, **Qc-5-Cu-dia** exhibits a different PXRD pattern and a change in color from blue to purple (Figure S9) whereas **Qc-5-Ni-dia** transforms between 1 and 14 days (Figure S10). In contrast, **Qc-5-Cu-sql-α** and **Qc-5-Cu-sql-β** maintain structural integrity for the duration of stability test (Figure S11) and **Qc-5-Cu-sql-β** remains unchanged after being soaked in water for 21 days (Figure 2). We observed negligible weight increase after **Qc-5-Cu-sql-β** was exposed to a moist N_2 stream during gravimetric experiments (Figure S47). CO_2 sorption experiments verified that the sorption performance of **Qc-5-Cu-sql-β** is unaffected by the stability tests (Figure S22). Such stability to water and water vapor contrasts with many well-known MOFs that are subject to degradation under similar conditions.[21] We attribute such good hydrolytic stability to the coordinatively saturated Cu^{2+} cations in **Qc-5-Cu-sql-β** (Figure S4).

Water vapor can negatively impact uptake and long-term performance of physisorbents.[22] Temperature-programmed desorption (TPD) experiments were conducted to gauge the performance of **Qc-5-Cu-sql-β** under equilibrium conditions after exposure to a simulated flue-gas mixture containing water vapor, CO_2, and N_2. The TPD studies suggest that the performance of **Qc-5-Cu-sql-β** is unaffected by the introduction of moisture to the flue-gas stream since a minimal amount of water adsorbed. Based on the amounts of adsorbed CO_2 and H_2O and the initial ratio of CO_2 and H_2O in the inlet gas mixture, the CO_2/H_2O selectivity (S_{CW}) was calculated to be 1.35 after exposing the sample to a simulated flue-gas mixture for 1 h (Figure S44–S46). This is much higher than several benchmark materials (0.17 for MgDOBDC, 0.02 for HKUST-1, 0.27 for SIFSIX-3-Ni and 0.05 for Zeolite 13X) studied under the same conditions.[19]

Real-time dynamic breakthrough experiments were conducted using CO_2/N_2 (wet and dry) and CO_2/CH_4 gas mixtures. Gas mixtures that simulate flue-gas streams (15% CO_2/ 85% N_2, or 50% CO_2/ 50% CH_4) were passed through a fixed-bed reactor (8 mm Ø) filled with **Qc-5-Cu-sql-β**. The sample was pre-treated by heating to 100°C in a flow of helium gas to release atmospheric impurities and then cooled to room temperature. Evolved gas components were continuously monitored using mass spectrometry (MS, see Supporting Information). CO_2 breakthrough occurs at 121, 112, and 51 min, for dry CO_2/N_2, wet CO_2/N_2, and dry CO_2/CH_4, respectively. Conversely, N_2 and CH_4 pass through the sample bed rapidly (Figure 5). The adsorption capacity of **Qc-5-Cu-sql-β** for CO_2 was calculated to be 44.4, 41.4, and 46.5 $cm^3 g^{-1}$, for the three gas mixtures, respectively, correlating well with CO_2 uptake (48.4 $cm^3 g^{-1}$ at 293 K, 1 bar) from single-component isotherms. These data indicate that the carbon capture capacity is independent of the gas mixture composition.

To conclude, sieving of CO_2 from gas mixtures was achieved in the 2D coordination network **Qc-5-Cu-sql-β** thanks to its 3.3 Å channels. This facile to prepare material is moisture-stable and its performance is largely unaffected by the presence of water vapor. This sweet spot in terms of pore-size and pore-chemistry was achieved by exploiting the phenomenon of supramolecular isomerism, which to our knowledge has not yet been exploited to control pore size. Molecular sieving, while difficult to achieve, offers great promise in terms of extremely high selectivity if membranes can be developed. Future work will focus on creating membranes[10d] from **Qc-5-Cu-sql-β**, for which 2D networks should be predisposed.[23]

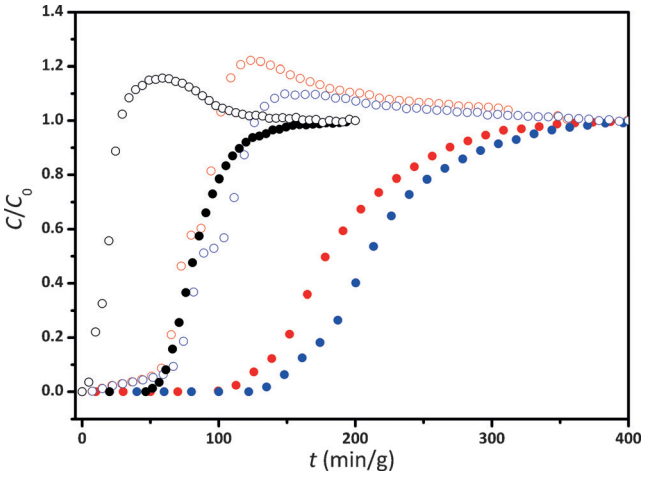

Figure 5. Breakthrough curves for **Qc-5-Cu-sql-β** in a fixed-bed under flow (2 $cm^3 min^{-1}$) of CO_2/CH_4 (50:50, black) and CO_2/N_2 (15:85) gas mixtures under dry (blue) and wet (red) conditions (75% humidity). filled symbols = CO_2, open symbols = CH_4 or N_2.

Acknowledgements

M.J.Z. acknowledges SFI (13/RP/B2549), and B.S. acknowledges the National Science Foundation (Award No. CHE-1152362). Computational resources were made available by XSEDE Grant No. TG-DMR090028. The use of the services provided by Research Computing at the University of South Florida is also acknowledged. J.-P.Z. and X.-M.C. acknowledge the NSFC (21225105 and 21290173). We also acknowledge Teresa Curtin (UL) for use of her dynamic breakthrough and temperature programmed desorption (TPD) equipment.

Keywords: CO_2 separation · gas sorption · molecular sieving effect · stability · supramolecular isomerism

How to cite: *Angew. Chem. Int. Ed.* **2016**, *55*, 10268–10272
Angew. Chem. **2016**, *128*, 10424–10428

[1] R. Monastersky, *Nature* **2013**, *497*, 13–14.
[2] a) M. Tagliabue, D. Farrusseng, S. Valencia, S. Aguado, U. Ravon, C. Rizzo, A. Corma, C. Mirodatos, *Chem. Eng. J.* **2009**, *155*, 553–566; b) S. Cavenati, C. A. Grande, A. E. Rodrigues, *J. Chem. Eng. Data* **2004**, *49*, 1095–1101.
[3] J. J. Perry IV, J. A. Perman, M. J. Zaworotko, *Chem. Soc. Rev.* **2009**, *38*, 1400–1417.

[4] a) S. Kitagawa, R. Kitaura, S.-I. Noro, *Angew. Chem. Int. Ed.* **2004**, *43*, 2334 – 2375; *Angew. Chem.* **2004**, *116*, 2388 – 2430; b) S. R. Batten, S. M. Neville, D. R. Turner, *Coordination Polymers*: *Design*, *Analysis and Application*, RSC, Cambridge, **2009**.
[5] a) D. Farrusseng, *Metal-Organic Frameworks*: *Applications from Catalysis to Gas Storage*, Wiley-VCH, Weinheim, **2011**; b) L. R. MacGillivray, *Metal-Organic Frameworks*: *Design and Applications*, Wiley, Hoboken, **2010**.
[6] B. Moulton, M. J. Zaworotko, *Chem. Rev.* **2001**, *101*, 1629 – 1658.
[7] a) M. Eddaoudi, J. Kim, N. Rosi, D. Vodak, J. Wachter, M. O'Keeffe, O. M. Yaghi, *Science* **2002**, *295*, 469 – 472; b) O. M. Yaghi, M. O'Keeffe, N. W. Ockwig, H. K. Chae, M. Eddaoudi, J. Kim, *Nature* **2003**, *423*, 705 – 714.
[8] a) P. Nugent, Y. Belmabkhout, S. D. Burd, A. J. Cairns, R. Luebke, K. Forrest, T. Pham, S. Q. Ma, B. Space, L. Wojtas, M. Eddaoudi, M. J. Zaworotko, *Nature* **2013**, *495*, 80 – 84; b) O. Shekhah, Y. Belmabkhout, Z. J. Chen, V. Guillerm, A. Cairns, K. Adil, M. Eddaoudi, *Nat. Commun.* **2014**, *5*, 4228; c) M. H. Mohamed, S. K. Elsaidi, L. Wojtas, T. Pham, K. A. Forrest, B. Tudor, B. Space, M. J. Zaworotko, *J. Am. Chem. Soc.* **2012**, *134*, 19556 – 19559.
[9] B. L. Chen, S. Q. Ma, E. J. Hurtado, E. B. Lobkovsky, H.-C. Zhou, *Inorg. Chem.* **2007**, *46*, 8490 – 8492.
[10] a) D. N. Dybtsev, H. Chun, S. H. Yoon, D. Kim, K. Kim, *J. Am. Chem. Soc.* **2004**, *126*, 32 – 33; b) J. W. Yoon, S. H. Jhung, Y. K. Hwang, S. M. Humphrey, P. T. Wood, J.-S. Chang, *Adv. Mater.* **2007**, *19*, 1830 – 1834; c) M. Dincă, J. R. Long, *J. Am. Chem. Soc.* **2005**, *127*, 9376 – 9377; d) Y. Peng, Y.-S. Li, Y.-J. Ban, H. Jin, W.-M. Jiao, X.-L. Liu, W.-S. Yang, *Science* **2014**, *346*, 1356 – 1359; e) X.-C. Huang, J.-P. Zhang, X.-M. Chen, *Chin. Sci. Bull.* **2003**, *48*, 1531 – 1534; f) K. S. Park, Z. Ni, A. P. Côté, J. Y. Choi, R.-D. Huang, F. J. Uribe-Romo, H. K. Chae, M. O'Keeffe, O. M. Yaghi, *Proc. Natl. Acad. Sci. USA* **2006**, *103*, 10186 – 10191.
[11] Z.-J. Zhang, Z.-Z. Yao, S. C. Xiang, B. L. Chen, *Energy Environ. Sci.* **2014**, *7*, 2868 – 2899.
[12] a) A. Anson, C. C. H. Lin, S. M. Kuznicki, J. A. Sawada, *Chem. Eng. Sci.* **2009**, *64*, 3683 – 3687; b) K. Morishige, *J. Phys. Chem. C* **2011**, *115*, 9713 – 9718; c) L. T. Du, Z. Y. Lu, K. Y. Zheng, J. Y. Wang, X. Zheng, Y. Pan, X. Z. You, J. F. Bai, *J. Am. Chem. Soc.* **2013**, *135*, 562 – 565; d) L. Hou, W. J. Shi, Y. Y. Wang, Y. Guo, C. Jin, Q. Z. Shi, *Chem. Commun.* **2011**, *47*, 5464 – 5466; e) W. M. Bloch, R. Babarao, M. R. Hill, C. J. Doonan, C. J. Sumby, *J. Am. Chem. Soc.* **2013**, *135*, 10441 – 10448.
[13] J.-P. Zhang, X.-C. Huang, X.-M. Chen, *Chem. Soc. Rev.* **2009**, *38*, 2385 – 2396.
[14] A. L. Spek, *J. Appl. Crystallogr.* **2003**, *36*, 7 – 13.
[15] A. L. Myers, J. M. Prausnitz, *AIChE J.* **1965**, *11*, 121 – 127.
[16] a) K. Sumida, D. L. Rogow, J. A. Mason, T. M. McDonald, E. D. Bloch, Z. R. Herm, T.-H. Bae, J. R. Long, *Chem. Rev.* **2012**, *112*, 724 – 781; b) J.-R. Li, Y. G. Ma, M. C. McCarthy, J. L. Sculley, J. M. Yu, H.-K. Jeong, P. B. Balbuena, H.-C. Zhou, *Coord. Chem. Rev.* **2011**, *255*, 1791 – 1823; c) J.-B. Lin, W. Xue, J.-P. Zhang, X.-M. Chen, *Chem. Commun.* **2011**, *47*, 926 – 928. See also Table S3 and references therein.
[17] Q.-M. Wang, D. Shen, M. Bülow, M. Ling Lau, S. Deng, F. R. Fitch, N. O. Lemcoff, J. Semanscin, *Microporous Mesoporous Mater.* **2002**, *55*, 217 – 230.
[18] J. An, N. L. Rosi, *J. Am. Chem. Soc.* **2010**, *132*, 5578 – 5579.
[19] J. Kim, S.-T. Yang, S. B. Choi, J. Sim, J. Kim, W.-S. Ahn, *J. Mater. Chem.* **2011**, *21*, 3070 – 3076.
[20] a) A. Kumar, D. G. Madden, M. Lusi, K.-J. Chen, E. A. Daniels, T. Curtin, J. J. Perry IV, M. J. Zaworotko, *Angew. Chem. Int. Ed.* **2015**, *54*, 14372 – 14377; *Angew. Chem.* **2015**, *127*, 14580 – 14585; b) H.-B. Kim, *Handbook of Stability Testing in Pharmaceutical Development: Regulations*, *Methodologies*, *and Best Practices*, Springer, New York, **2009**.
[21] a) J. Canivet, A. Fateeva, Y. M. Guo, B. Coasne, D. Farrusseng, *Chem. Soc. Rev.* **2014**, *43*, 5594 – 5617; b) N. C. Burtch, H. Jasuja, K. S. Walton, *Chem. Rev.* **2014**, *114*, 10575 – 10612.
[22] a) S. Keskin, T. M. van Heest, D. S. Sholl, *ChemSusChem* **2010**, *3*, 879 – 891; b) T. C. Drage, C. E. Snape, L. A. Stevens, J. Wood, J. W. Wang, A. I. Cooper, R. Dawson, X. Guo, C. Satterley, R. Irons, *J. Mater. Chem.* **2012**, *22*, 2815 – 2823; c) J. A. Mason, T. M. McDonald, T.-H. Bae, J.-E. Bachman, K. Sumida, J. J. Dutton, S. S. Kaye, J. R. Long, *J. Am. Chem. Soc.* **2015**, *137*, 4787 – 4803.
[23] Single-crystal data (CCDC numbers: 1470735, 1470736, 1470737, 1470738, 1470739, and 1470740) for this article can be obtained free of charge from The Cambridge Crystallographic Data Centre via www.ccdc.cam.ac.uk/data_request/cif.

Received: April 22, 2016
Published online: July 21, 2016

